Applied Catalysis B: Environmental 185 (2016) 272–280

Contents lists available at ScienceDirect

Applied Catalysis B: Environmental

journal homepage: www.elsevier.com/locate/apcatb

NbO_x/SiO_2 in the gas-phase Beckmann rearrangement of cyclohexanone oxime to ε-caprolactam: Influence of calcination temperature, niobia loading and silylation post-treatment

M.M. Maronna[a,b,*,1], E.C. Kruissink[a], R.F. Parton[a], J.T. Tinge[a], F. Soulimani[c], B.M. Weckhuysen[c], W.F. Hoelderich[d,1]

[a] DSM Chemical Technology R&D B.V., Urmonderbaan 22, 6167 RD Geleen, The Netherlands
[b] TU Dortmund, Lehrstuhl für Technische Chemie B, Emil-Figge-Straße 66, 44227 Dortmund, Germany
[c] Utrecht University, Inorganic Chemistry and Catalysis Group, Debye Institute for Nanomaterials Science, Universiteitsweg 99, 3584 CG Utrecht, The Netherlands
[d] TCHK Consultancy, 67227 Frankenthal, Germany

ARTICLE INFO

Article history:
Received 10 August 2015
Received in revised form 6 December 2015
Accepted 10 December 2015
Available online 12 December 2015

Keywords:
Gas-phase Beckmann rearrangement
Cyclohexanone oxime to ε-caprolactam
Amorphous niobia on silica catalyst
Raman spectroscopy
Silylation post-treatment

ABSTRACT

NbO_x/SiO_2 catalyst materials prepared by the incipient wetness impregnation method were studied in the industrially relevant gas-phase Beckmann rearrangement of cyclohexanone oxime to ε-caprolactam. The catalytic experiments were carried out in a fixed bed reactor system at atmospheric pressure. Results have been complemented with Raman and FT-IR spectroscopy as well as N_2 physisorption measurements. Optimal catalytic results were observed for a catalyst calcination temperature of 600 °C and a niobia loading of 0.3 wt.%. Raman spectroscopy revealed that isolated tetrahedral mono-oxo NbO_4 surface species most probably play a key role in the catalytic reaction. Very positive effects were achieved by applying a catalyst silylation post-treatment. Firstly, the catalytic long-term stability increased very substantially as a consequence of a decreased coke deposition on the catalyst surface. Secondly, the harmful effect of water on catalytic performance was strongly suppressed even to such an extent that water could be added to the feed to enhance catalytic long-term stability. Cyclohexanone oxime conversion and ε-caprolactam selectivity could be maintained at constant high values >99% and around 95% respectively, for 26 h time-on-stream. Finally, considering the Sumitomo gas-phase Beckmann rearrangement process as a benchmark, we made a rough comparison between the catalytic performances of our niobia/silica catalyst and the silicalite catalyst used by Sumitomo.

1. Introduction

The gas-phase Beckmann rearrangement (hereinafter referred to as GPBR) of cyclohexanone oxime towards ε-caprolactam has been investigated since the 1940's. The main objective of these research efforts was to avoid the disadvantages of the conventional homogeneously sulphuric acid/oleum catalysed process where ammonium sulphate is a very substantial by-product [1]. First, dehydrating oxides, such as silica, alumina, titania, magnesia and tungsten oxide [2,3], were investigated and later several oxides loaded with acidic salts and/or phosphoric acid [4–6] or boron oxide [7] were tested for this important catalytic reaction. After the development of synthetic zeolites, many investigations were executed with several types of pure and doped zeolites and later also with mesoporous molecular sieves (MMS). Profound experimental results using fluidized bed technology for the vapour-phase Beckmann rearrangement have been reported by Hoelderich and his group [1,8–11]. After all, the first company that commercialized a GPBR process was Sumitomo Chemicals Co. Ltd. in 2003, using a relatively expensive highly siliceous MFI zeolite (silicalite) as catalyst in a fluidized bed reactor system with continuous regeneration [12–15].

Niobium (Nb) and tantalum (Ta) containing catalyst materials for GPBR [16,17] were first investigated by Ushikubo et al. utilizing TaO_x/SiO_2, bulk tantalic acid, bulk niobic acid and bulk niobia. Also VO_x/SnO_2 has been used [18], completing the group V metal

* Corresponding author at: TU Dortmund, Lehrstuhl für Technische Chemie B, Emil-Figge-Straße 66, 44227 Dortmund, Germany.
E-mail address: marius.maronna@tu-dortmund.de (M.M. Maronna).
[1] Formerly: RWTH Aachen, Lehrstuhl für Technische Chemie und Heterogene Katalyse, Worringerweg 1, 52074 Aachen, Germany.

http://dx.doi.org/10.1016/j.apcatb.2015.12.014
0926-3373/

oxides. Nb-doped catalysts were investigated more intensively in GPBR [14–26]. Recently, it was found that Nb-MCM-41, Nb-SBA-15, Nb-HMS and Nb-Beta are suitable catalyst materials for the GPBR applied in a fixed bed reactor system resulting in high cyclohexanone oxime conversion and ε-caprolactam selectivity [22,23]. Furthermore, Hoelderich et al. showed that a relatively cheap NbO_x/SiO_2 exhibited a similar high catalytic performance compared to the Nb-doped zeolitic and mesoporous materials [24,25] and additionally performed activity in cyclohexanone ammoximation [26]. Thus, this amorphous NbO_x/SiO_2 material is a promising alternative for the more expensive zeolitic and MMS compounds. However, regarding to industrial applicability, there are several unexplored areas of the NbO_x/SiO_2 system left. With respect to reaction conditions, no data are available on the catalytic performance at higher total reactor pressure, different cyclohexanone oxime partial pressures at various reaction temperatures, higher catalyst loads, different linear gas velocities and the utilization of substrate additives. Furthermore, regarding to catalyst properties, results with different Nb_2O_5 loadings on silica, calcination temperatures, catalyst post-treatments, such as silylation, and the influence of the catalyst particle diameter are missing.

In view of the above considerations, in this work the effect of calcination temperature and niobia loading of the NbO_x/SiO_2 catalyst materials on their GPBR performance will be discussed. Furthermore, the effect of catalyst silylation and water addition to the feed on the catalytic long-term stability will be shown. The performed catalytic experiments have been complemented with Raman and FT-IR spectroscopy as well as N_2 physisorption measurements on the catalyst materials prepared.

2. Experimental

2.1. Catalyst preparation

For the preparation of the catalysts silica support materials were used with the product names DAVICAT SI 1151 and DAVICAT SI 1410 (Grace Davison). The BET surface areas of these silicas amount to 288 and 36 $m^2 g^{-1}$ and the BJH average pore diameters are 11.5 and ~100 nm, respectively. It should be remarked that DAVICAT SI 1151, used for the preparation of most catalysts, contains minor concentrations of impurities (measured with ICP-OES): sodium (640 ppm), potassium (380 ppm), aluminium (90 ppm) and iron (30 ppm). After crushing and sieving to obtain the desired fraction, the silica was dried at 150 °C for 3 h. The dried silica was loaded via the incipient wetness impregnation method with an appropriate amount of an ethanol (VWR, 99%, dried) solution of $Nb(OEt)_5$ (Sigma–Aldrich, 98%). After short intensive mixing in a rotary evaporator, resulting in a homogeneous wetting of the particles, vacuum was applied followed by ventilation (repeated three times) to push the precursor solution deep into the pore system of the carrier material. Then, the loaded silica was calcined in static air at a predetermined temperature (range: 400 °C ≤ T ≤ 800 °C) for 15 h (heating rate from RT to target temperature 2 °C min^{-1}) and finally cooled down slowly to RT again. For a part of the samples, directly after the calcination a silylation post-treatment was applied. To this end, the catalyst was refluxed at 125 °C while stirring in pure hexamethyldisilazane (HMDS, VWR, 99%) for 6 h, followed by filtration, washing thoroughly with dry toluene (VWR, 99%, dried) and drying at 150 °C under vacuum for 3 h. In the following, catalyst materials, which were post-treated with HMDS, are called "silylated". Results to be discussed on the effects of calcination temperature and niobia loading were all obtained using silylated catalysts. Reason to execute a silylation treatment was that in literature on GPBR with zeolite catalysts better ε-caprolactam selectivity was observed due to the etherification of terminal silanol groups with methanol [27] or blocking the terminal silanols via reaction with trimethylchlorosilane (TMCS) [28]. In the present work it was decided to block the isolated silanol groups with thermally very stable trimethylsilyl groups, too, via the reaction with HMDS.

2.2. Catalyst characterization

Nitrogen adsorption isotherms were measured with a Micromeritics Gemini VII 2390 Surface Analyser. The samples were evacuated at 300 °C for 2 h and cooled down to −196 °C under vacuum. To obtain the adsorption–desorption isotherms, the nitrogen pressure was varied in the relative pressure range (P/P_0) between 0.01 and 0.96. Brunauer–Emmett–Teller (BET) surface areas were calculated from the part of the adsorption isotherm between 0.05 and 0.25 P/P_0. Mesopore volumes and diameters were calculated from the desorption branch of the isotherm using the Barrett–Joyner–Halenda (BJH) method; micropore volumes were obtained from the t-plot.

The elemental analysis to determine the niobia loading of the catalysts was executed using inductively coupled plasma optical emission spectroscopy (ICP-OES) utilizing a Thermo Scientific iCAP6500 system. In order to perform the measurements the catalysts (~0.2 wt.%) were dissolved in an aqueous solution of hydrofluoric and nitric acid.

Raman spectra were recorded with a Kaiser RXN1 spectrometer using a green laser (λ = 514 nm, P = 100 mW, 5 s exposure time, 20 accumulations) and a non-contact 5.5" objective for laser focussing and collecting the scattered radiation. The catalyst was located in a quartz glass reactor with connections to feed gases. The spectra were recorded under flowing N_2 atmosphere at 400 °C reactor temperature under dehydrated conditions.

FT-IR spectra were recorded with a PerkinElmer Spectrum One spectrometer including a stainless steel measuring cell with KBr windows and connections to feed gases. The materials were pressed into cyclic self-supporting wafers (~10 mg material pressed at 8000 kg and RT, ø = 8 mm) and fixed into the holder of the measuring cell. The wafers were heated out at 200 °C for 2 h under flowing N_2 atmosphere before spectra were recorded.

2.3. Catalytic testing

2.3.1. General description of catalytic testing unit and testing procedure

Catalytic testing was performed in a tubular plug flow fixed bed reactor system which is outlined in Fig. S1. A HPLC two piston pump (P1) feeds the substrate solution through a capillary (to create the necessary pressure drop) to the stainless steel spiral tube evaporator (E1, length 650 mm, inner diameter 6 mm), followed by a vertical tubular fixed bed reactor (R1, length 500 mm, inner diameter of 21 mm). The evaporator and the reactor were located in one single tube oven (O1). The temperatures of the three separate heating segments of the oven were controlled with one thermocouple in the evaporator tube and two thermocouples in the catalyst bed. Evaporator and reactor were kept on the same temperature (400 °C). The reactor outlet tube was kept constant at 300 °C and ended in a double walled glass condensing system (C1) cooled down to −20 °C with cryostats to quench the product gas mixture. The liquid product mixture was constantly pumped off the condenser bottom with a membrane pump (P2). The reactor inlet pressure (p_{in}) was kept constant, therefore the pressure was measured (at PT1) and if necessary corrected by decreasing the reactor outlet pressure (p_{out}, measured at PT2) via a dynamically acting vacuum pump (P3) connected to the condensing system. So the reactor inlet pressure was always higher than its outlet pressure. Additionally N_2 gas could be dosed into the system in front of the evaporator via a mass flow controller (MFC1). If necessary, the

catalyst bed height was always adapted to 80 times the average catalyst particle diameter by homogeneous dilution with silicon carbide (SiC) particles. In front of the catalyst bed an additional bed of pure SiC particles with a height of 20 mm was placed in order to prepare almost plug flow conditions of the reactant gas before it contacted the catalyst bed. The average bead diameter of catalyst and SiC particles was equal and did not exceed one tenth of the reactor diameter. Each experiment was started up by flushing the reactor system with nitrogen (180 l h^{-1}) while the evaporator and reactor were heated up. After the catalyst bed reached the final temperature the nitrogen flow was adapted to the experimental set point and substrate was pumped into the system.

The average total gas volume flow $\left(F^{g}_{total}\right)$ was calculated via the ideal gas law including the total molar input flow of substrate components including N_2 $\left(F^{n}_{total} = \sum_{i}^{n} F^{n}_{i}\right)$, the average reactor pressure $\left(\overline{p_r} = \frac{(p_{in}+p_{out})}{2}\right)$ and the reactor temperature (T_r), following Eq. (1).

$$F^{g}_{total} = \frac{F^{n}_{total} \times R \times T_r}{\overline{p_r}} \quad (1)$$

The substrate component partial pressures (p_i) in the gas phase in front of the catalyst bed were derived from the molar flow fraction of a component and the reactor inlet pressure (p_{in}), according to Eq. (2).

$$p_i = \frac{F^{n}_{i} \times p_{in}}{F^{n}_{total}} \quad (2)$$

The residence time in the catalyst bed volume (τ) was calculated as ratio of the pure catalyst bed volume ($V_{catalyst}$) to the average total gas volume flow $\left(F^{g}_{total}\right)$. The catalyst load expressed as weight hourly space velocity (WHSV) was calculated as quotient of cyclohexanone oxime mass flow $\left(F^{m}_{oxime}\right)$ pumped into the reactor to the catalyst mass in the reactor bed ($m_{catalyst}$).

2.3.2. Substrate and product analysis

All substrate and product analysis were carried out on a Hewlett Packard 5890 series 2 gas chromatograph (GC) with a Hewlett Packard 7673 auto sampler system (injector and controller). The digital data recording (sampling rate of 20 Hz) and peak integration were done with the Atlas software version 8.20.2.7047 of the Thermo Electron Corporation. To quantify the reaction products the detector was calibrated via external calibration method for each substance. Nitrogen was used as carrier gas (0.1 MPa, split ratio 1:50), 1 μl product solution was injected into the evaporator (250 °C) and led over a capillary column (30 m × 0.25 mm × 1 μm, VF WAX, CP9206, Agilent Technologies) ending up in a FID (flame ionization detector, 250 °C) for substance detection. For an optimal separation of the substance mixture a temperature program was used (5 min isotherm at 50 °C, heating up to 240 °C with 10 °C min^{-1}, 17 min isotherm at 240 °C).

The liquefied product mixture was collected after a certain sampling time ($t_{sampling}$), normally 60 min. Amounts of consumed substrate and collected product during sampling time were determined by weighing ($m^{substrate}$ and $m^{product}$). The substrate solution as well as the product solutions were analysed by the GC method to quantify the fed cyclohexanone oxime amount $\left(n^{fed}_{oxime}\right)$, the unconverted cyclohexanone oxime amount $\left(n^{product}_{oxime}\right)$ and product amounts $\left(n^{product}_{i}\right)$, all quantities referring to the sampling time. Cyclohexanone oxime conversion (X) and product selectivities (S_i) were calculated according to Eqs. (3) and (4), respectively.

$$X\,[-] = 1 - \frac{n^{product}_{oxime}}{n^{fed}_{oxime}} \quad (3)$$

$$S_i\,[-] = \frac{n^{product}_{i}}{n^{fed}_{oxime} - n^{product}_{oxime}} \quad (4)$$

Reaction rates were calculated according to Eq. (5) including $t_{sampling}$ and the catalyst mass.

$$r\left[mmol \times kg^{-1} \times s^{-1}\right] = \frac{\frac{n^{fed}_{oxime} - n^{product}_{oxime}}{t_{sampling}}}{m_{catalyst}} \quad (5)$$

Presented data were taken from 5 h time-on-stream (TOS) results of each single experiment, unless otherwise indicated. The reason for this was that at this time-on-stream the cyclohexanone oxime conversion, ε-caprolactam selectivity and reaction rate were on a stable level. Carbon balances were always between 93 and 97%. Losses are mainly due to incomplete condensation of the gaseous product and to a less extent to deposited material (coke) on the catalyst and measuring uncertainties. The presented results are not corrected for blank effects (activity of empty reactor). However, as will be discussed in Section 3.2, the activity in GPBR measured for the unloaded silica support (DAVICAT SI 1151) is hardly significant. In view of this a correction for the activity of the empty reactor is not necessary.

2.4. Remarks on parameter selection

2.4.1. Total pressure and ethanol partial pressure

All experiments were carried out at a reactor inlet pressure ranging from 90 to 120 kPa (absolute). These relatively high pressures are more favourable for industrial application than the much lower reactor pressure (10 kPa) often applied in previous work on the same catalyst system [22–26]. In our experiments ethanol was used as solvent for cyclohexanone oxime. It should be mentioned that methanol or ethanol are often reported as solvents in GPBR for very different catalytic systems [8,29–33]. Since both cyclohexanone oxime and ethanol partial pressures cannot be increased too much due to increasing side reactions, toluene was utilized as inert and cheap component to make up the higher total pressure. The effect of the ethanol partial pressure will be discussed more extensively in a subsequent paper about the kinetics of GPBR over these Nb-catalysts [34]. Here it is sufficient to remark that no or just a very small effect on catalytic performance was observed for the ethanol to cyclohexanone oxime molar ratios between 3 and 8 used in the present work.

2.4.2. Linear gas velocity and particle size

To check for film diffusion and pore diffusion limitations, some tests were performed with different values of the linear gas velocity and particle size (all other parameters being constant). The catalyst based on the DAVICAT SI 1151 silica carrier had a niobia loading of 0.01 wt.%. It turned out that reaction rates did not increase anymore for superficial gas velocities ≥0.6 m s^{-1} (corresponding to ≥800 l h^{-1} total volume flow in our case) [34]. The variation of particle diameter for an optimized linear gas velocity (1000 l h^{-1}) and fixed other parameters showed that activity is constant for particle diameters of 0.6 mm and lower [34]. Thus, to avoid film and pore diffusion limitations, total gas volume flow should be ≥800 l h^{-1} and catalyst particle diameter should be ≤0.6 mm. Most of the experiments reported in this publication meet these requirements. Only the topics presented in Sections 3.3 and 3.4

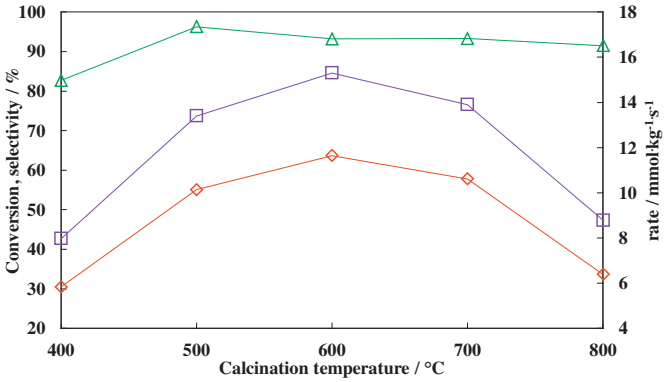

Fig. 1. Catalytic performances, as expressed by the cyclohexanone oxime conversion (◇), ε-caprolactam selectivity (△) and reaction rate (□), dependent on the catalyst (0.01 wt.% Nb_2O_5 on DAVICAT SI 1151 silica, 0.55–0.75 mm particle fraction, silylated) calcination temperature. Reaction conditions: T_r: 400 °C, p_{in}: 100 kPa, F^g_{total}: 1000 l h^{-1}, τ: 0.025 s, p_{EtOH}: 10 kPa, p_{oxime}: 1.5 kPa, p_{Tol}: 88.5 kPa, $m_{cat.}$: 2.8 g, $V_{cat.}$: 7 cm^3, WHSV: 10.8 h^{-1}, and 8 h time-on-stream.

were investigated before full optimization of the reaction parameters. However, the results are used in a strictly comparative way and possible deviations in the absolute values will not affect the conclusions.

3. Results and discussion

3.1. Effect of catalyst calcination temperature

Fig. 1 presents catalyst activity and selectivity as a function of calcination temperature. It follows that there is an optimum in activity for 600 °C calcination temperature. The ε-caprolactam selectivity is much less dependent on the calcination temperature, but increases significantly from 400 °C to 500 °C, and then decreases only by a minor amount from 600 °C to 800 °C. The total by-product selectivity is for the greater part due to unidentifiable compounds, the selectivity to the latter ranging from about 2% (800 °C calcination temperature) to 10.8% (400 °C calcination temperature). The main identified by-products are cyclohexanone and hexanenitrile, both ranging from about 0.5% (600 °C calcination temperature) to about 2.0% (400 °C calcination temperature). More data on the by-product composition can be found in the Supporting information, Fig. S2.

N_2 physisorption data of the catalyst materials prepared are summarized in Table 1, illustrating that high calcination temperatures have only a small effect on the textural properties, i.e. that changes of surface area, pore size and pore volume cannot be the reason for the catalytic effects observed. But for 800 °C both BET surface area and pore volume of the Nb-containing catalysts are significantly higher than that of the unloaded support, indicating that the silica support is stabilized by the presence of niobia at the surface.

Table 2
Raman band assignments for Nb_2O_5/SiO_2 catalysts based on literature data [35–45].

Wavenumber/cm^{-1}	Assignment
795	Silica network
930	Oligomeric Nb—O—Nb
965	Isolated surface Si—OH stretching vibration
981	Nb=O stretching vibration
994, 1047	Transverse optical stretch of silica network
1119, 1155	Longitudinal optical stretch of silica network

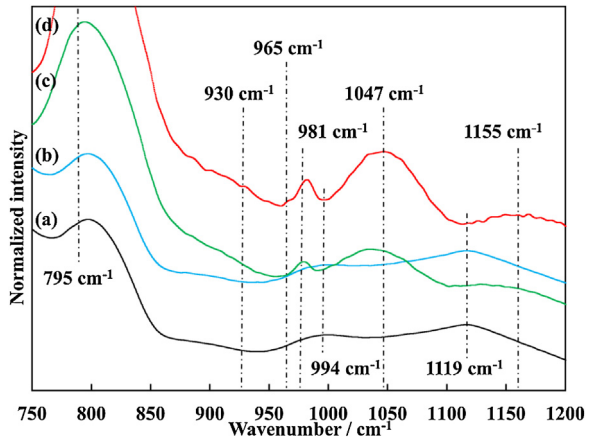

Fig. 2. Raman spectra of the unsilylated pure silica material (DAVICAT SI 1151) calcined at 600 °C (a) and the unsilylated model catalysts (modifications of catalyst K in Table 3) containing 1.8 wt.% Nb_2O_5 and calcined at 400 °C (b), 600 °C (c) and 800 °C (d). The spectra were measured in-situ under dehydrated conditions under N_2 atmosphere and at 400 °C in a quartz reactor.

To support the interpretation of the differences in catalytic performance Raman spectra were recorded. For this, model catalysts with 1.8 wt.% niobia on the DAVICAT SI 1151 silica calcined at 400, 600 and 800 °C were synthesized (modifications of catalyst K in Table 3). A higher niobia loading turned out to be necessary because of the sensitivity of the applied Raman spectrometer. Unsilylated samples had to be used, because fluorescence (even after 24 h decay time) of the silylated model catalysts made measurements impossible. The in-situ Raman spectra were recorded under dehydrated conditions at 400 °C under flowing N_2 atmosphere and are shown in Fig. 2 . Table 2 presents the spectral assignments as agreed upon in literature [35–45].

The Raman spectra of the catalysts calcined at 600 °C and 800 °C, exhibit a distinct peak at 981 cm^{-1} which is assigned to the Nb=O vibration of an isolated tetrahedral NbO_4 mono-oxo surface species [35–38]. This peak is neither visible for the catalyst calcined at 400 °C, nor any other NbO_x surface groups were observed for this catalyst material. Assuming a key role in catalytic performance

Table 1
Textural properties of the DAVICAT SI 1151 silica support and the related 0.01 wt.% niobia on DAVICAT SI 1151 silica catalyst (0.55–0.75 mm particle fraction), both calcined at different temperatures.

Support/catalyst	Calcination temperature [°C]	BET surface area[a] [m^2 g^{-1}]	Micro pore volume [cm^3 g^{-1}]	BJH pore volume[b] [cm^3 g^{-1}]	BJH pore diameter[c] [nm]
DAVICAT SI 1151	400	287	0.005	1.2	12.4
0.01 wt.% Nb catalyst	400	292	0.009	1.1	12.6
DAVICAT SI 1151	600	273	0.002	1.1	12.1
0.01 wt.% Nb catalyst	600	280	0.003	1.0	12.2
DAVICAT SI 1151	800	224	0	0.8	11.4
0.01 wt.% Nb catalyst	800	242	0.002	0.9	12.4

[a] Brunauer–Emmett–Teller (BET) surface areas surface area.
[b] Barrett–Joyner–Halenda (BJH) cumulative pore volume (desorption).
[c] Barrett–Joyner–Halenda (BJH) average pore diameter (desorption).

Table 3
Catalytic performances of Nb_2O_5/SiO_2 catalysts measured after 8 h time-on-stream, for silylated catalyst materials with different niobia contents in the range of 0–2 wt.%. Silica carrier: DAVICAT SI 1151, particle fraction: 0.55–0.75 mm, calcination temperature: 600 °C.

Catalyst	C	D	E	F	G	H	I	J	K
Nb_2O_5 loading, aimed [wt.%]	0, pure silica	0.01	0.02	0.05	0.07	0.09	0.30	1.00	2.00
Nb_2O_5 loading, measured [wt.%]	0.00	0.009	0.019	0.052	0.072	0.089	0.300	0.930	1.788
ρ_A(Nb) [Nb nm^{-2}]	0	0.001	0.003	0.008	0.012	0.014	0.049	0.152	0.295
τ [s]	0.025	0.025	0.025	0.024	0.024	0.024	0.007	0.005	0.005
$m_{catalyst}$ [g]	2.8	2.8	2.8	2.8	2.8	2.8	0.8	0.6	0.6
$V_{catalyst}$ [cm^3]	6.9	6.9	6.9	6.9	6.9	6.9	2.1	1.4	1.4
WHSV [h^{-1}]	10.7	10.3	10.5	10.7	10.6	10.7	33.1	47.9	48.3
X_{8h} [%]	7.1	57.1	57.6	77.3	87.0	94.9	84.7	43.3	23.3
r [mmol kg$_{cat.}^{-1}$ s^{-1}]	1.9	14.3	14.9	20.1	22.5	24.4	69.0	50.9	27.7

for the NbO_4 species just mentioned (among others supported by literature where catalytic properties are reported for these surface niobia species [38]), the low activity after calcination at 400 °C can be explained by the absence or lower concentration of these sites. Probably, the surface species at low calcination temperature are niobic acid-like, partly connected to the surface e.g. $O_3Si{-}O{-}Nb{-}(OH)_4$. At higher calcination temperatures further bond formation to the silica surface and dehydration could occur, leading to species like $(O_3Si{-}O)_2{-}Nb{=}O({-}OH)$, and the final, most dehydrated $(O_3Si{-}O)_3{-}Nb{=}O$ species. Unfortunately, the weak Raman band of the Nb—O—Si links at ~865 cm^{-1} is overlapping with a broad silica band. Therefore, no correlation between peak intensity (=number of Nb—O—SiO_3 links) and calcination temperature can be established.

The substantially lower activity after calcination at 800 °C is difficult to explain. In the Raman spectrum, shown in Fig. 2, a weak peak at 930 cm^{-1} is visible, which can be assigned to Nb—O—Nb bonds. Possibly, at 800 °C mobility of surface Nb-atoms is sufficiently high to cause formation of oligomeric Nb—O—Nb species to a limited extent. This would decrease the number of isolated NbO_4 sites on the surface and thus decrease the activity. However, in view of the very low intensity of the observed Raman band we cannot be sure whether this is the correct explanation. Another possibility could be that due to restructuring of the surface as consequence of the increased mobility of the surface atoms, accessibility of the active sites has decreased.

Another feature in the Raman spectrum of the catalyst calcined at 800 °C (Fig. 2) is a shoulder observed at 965 cm^{-1} besides the Nb=O vibration. Such a band was assigned to the stretching vibration of isolated surface silanol groups [36,41–45]. Since the Raman measurements refer to unsilylated catalysts, the presence of isolated silanol groups is not surprising.

It is important to notice that the composition of identified by-products observed (with very low selectivity) in our experiments could be in agreement with the presence of low concentrations of isolated silanol groups remaining even after silylation. Several papers report the formation of a similar combination of by-products during the reaction of cyclohexanone oxime over siliceous catalysts containing (isolated) silanol groups [46–48].

3.2. Effect of Nb_2O_5 loading

In order to investigate the influence of different niobia contents, catalyst materials with different niobia loadings in the range of 0–2 wt.% were prepared (detailed properties see Table 3) and tested. The reaction conditions were the same as in Section 3.1 except changes in residence time to keep conversion well below 100% to ensure a meaningful comparison of the activities. The conversions and rates of reaction measured at 8 h time-on-stream are also included in Table 3.

It has to be taken into account that within this series the conversions are differing considerably (see Table 3) and therefore the reaction rates presented in Table 3 cannot be compared correctly as such. To obtain a comparable set of data, these rates should be corrected depending on kinetics. As will be published later on [34], for the low cyclohexanone oxime partial pressure (1.5 kPa) applied in these measurements activity follows first order kinetics with respect to cyclohexanone oxime partial pressure in very good approximation. Thus rates were recalculated, assuming first order kinetics, by multiplication by a factor of -ln(1-X)/X, with X being the cyclohexanone oxime conversion according to Eq. (3).

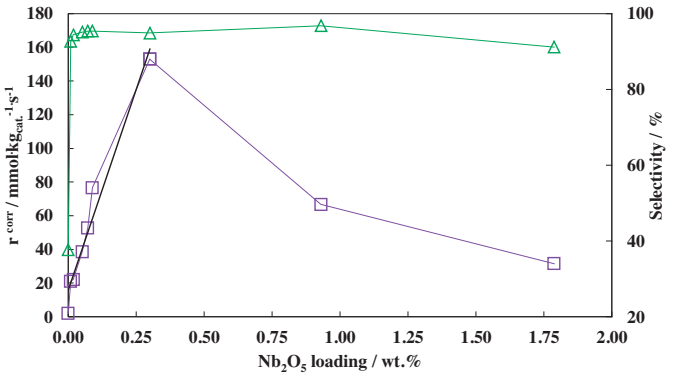

Fig. 3. Catalytic performances, as expressed by the corrected reaction rate (assuming 1st order kinetics, r^{corr}, □) and ε-caprolactam selectivity (Δ), as a function of the niobia loading (on DAVICAT SI1151 silica, 0.55–0.75 mm particle fraction, 600 °C calcination temperature, silylated) in the range of 0–2 wt.%. A line was fitted through the data points in the range of 0–0.3 wt.% niobia loading resulting in the following equation: r^{corr} = 477.8 wt.% Nb_2O_5 + 15.5 (R^2 = 96%). Reaction conditions: T_r: 400 °C, p_{in}: 100 kPa, F^g_{total}: 1000 l h^{-1}, p_{EtOH}: 10 kPa, p_{oxime}: 1.5 kPa, p_{Tol}: 88.5 kPa.

Fig. 3 presents the corrected reaction rates and the selectivities dependent on the niobia loading. It can be seen that the activity i.e. the reaction rate increases strongly with increasing niobia concentration up to 0.3 wt.% niobia where a sharp optimum is observed (see Fig. 3). For higher loadings exceeding 0.3 wt.% the activity decreases again. A line could be fitted through the rates between 0 and 0.3 wt.% niobia loading which indicates that the activity per niobium atom (6.4 molecules cyclohexanone oxime per Nb-atom, extracted from the slope) is constant for niobia loadings below 0.3 wt.%.

Without niobia (unloaded silica support, calcined and silylated) activity is hardly significant (r^{corr} = 1.87 mmol kg$_{cat.}^{-1}$ s^{-1}). Apparently, the presence of minor concentrations of impurities (mainly Na and K, see Section 2.1) does not lead to a significant catalytic activity. Furthermore, the ε-caprolactam selectivity is only 38% (leading to a ε-caprolactam productivity of 0.70 mmol kg$_{cat.}^{-1}$ s^{-1}). In contrast, for all niobia-containing catalysts selectivity is above 92% and hardly depending on niobia content, leading to a maximum ε-caprolactam productivity of 65.5 mmol kg$_{cat.}^{-1}$ s^{-1} for 0.3 wt.% niobia loading. This very strong increase of activity with increasing niobia loading in combination with the very low activity of pure silica shows that Nb-containing sites are essential for a very

Table 4
Weight increase and textural properties of fresh and used (after ≥46 h time-on-stream) catalysts (0.5 wt.% Nb_2O_5 niobia loading on DAVICAT SI 1410 silica, 1.0–0.85 mm particle fraction, 600 °C calcination temperature, L: unsilylated, L1: silylated).

Catalyst	L	L1
BET surface area of original (fresh) catalyst [m^2 g-1]	32	28
Catalyst weight increase after reaction [%]	53.9	41.2
Weight fraction of original catalyst in used catalyst	0.650	0.708
BET surface area after 46 h time-on-stream [m^2 g-1]	32	42
Fraction original catalyst to BET area after 46 h time-on-stream [m^2 $g_{used\ cat.}^{-1}$][a]	20.8	19.8

[a] BET surface area of original catalyst multiplied by weight fraction of original catalyst.

high catalytic performance. Regarding the nature of active sites of niobia/SiO_2 materials, it has been reported in literature that for low niobia concentrations below monolayer coverage, isolated tetrahedral mono-oxo NbO_4 groups are formed (see also previous Section). These groups contain a Nb=O bond and display catalytic properties [38–50]. A more detailed discussion about the nature of these sites will be published elsewhere [34].

It is remarkable that the optimum in activity is observed at such a relatively low niobia content (0.3 wt.% corresponding to a Nb-atom surface density of $\rho_A(Nb) = 0.05$ Nb nm^{-2}). Not many literature data are available for very low niobia surface concentrations. Jehng and Wachs found via spectroscopic investigations for silica as carrier material a loading limit of 2 wt.% niobia, corresponding to 0.3 Nb nm^{-2}, before oligomeric species occur [38–52]. In one of the publications of Ko and co-workers results for a series of three catalyst materials were ascribed to agglomeration of the niobia surface species [50]. Niobia surface densities for these three catalysts amount to 0.28, 0.54 and 1.55 Nb nm^{-2} resp. (calculated from the weight percentages and surface areas given by the authors). For the lowest NbO_x surface density (0.28 Nb nm^{-2}) the dispersion apparently was very high, since a high acidity was observed corresponding to about one acid site per niobium atom.

On the other hand, Datka et al. [53] found from FT-IR measurements with pyridine as probe molecule that for niobia loaded silica catalysts with 2–6 wt.% niobia, the concentration of Lewis acid sites amounts only to about 14% of the concentration of all Nb-atoms deposited on the carrier surface. Thus, in this case even for 2 wt.% niobia (corresponding to 0.3 Nb nm^{-2}) niobia dispersion is relatively low, due to the formation of bulk niobia particles. It has been acknowledged that the niobia-silica interaction is weak, and that therefore both the niobia concentration where oligomerization starts and niobia dispersion depend on the method of catalyst preparation [38]. The much lower activity in GPBR observed in this study (see Fig. 3) for the two highest niobia loadings (0.9 wt.%/0.15 Nb nm^{-2} and 1.8 wt.%/0.30 Nb nm^{-2}) suggests that in these cases agglomeration has occurred, resulting in a decreased concentration of isolated NbO_4 sites.

3.3. Comparing the catalytic performance of unsilylated and silylated catalyst

For a comparative study, catalyst L with a niobia loading of 0.5 wt.% was prepared (details see Table 4) using a silica with very large pores (DAVICAT SI 1410). Half of catalyst L was then post treated with HMDS in the following called L1.

The catalytic performance of both catalysts as a function of time-on-stream is compared in Fig. 4. During the first 6 h time-on-stream the ε-caprolactam selectivity increases, suggesting that in this phase non-selective sites are poisoned. The ε-caprolactam selectivities are increasing in a very similar way for the unsilylated and silylated catalyst, the main difference being the much lower

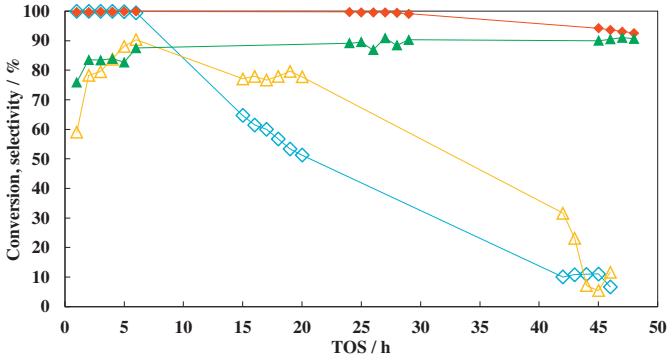

Fig. 4. Catalytic performance, as expressed by the cyclohexanone oxime conversion (◇, ◆) and ε-caprolactam selectivity (△, ▲), of an unsilylated (L, open symbols) and a silylated (L1, filled symbols) catalyst (0.5 wt.% Nb_2O_5 on DAVICAT SI 1410 silica, 1.0–0.85 mm particle fraction, 600 °C calcination temperature), as function of time-on-stream (TOS). Reaction conditions: T_r: 400 °C, p_{in}: 90 kPa, F^g_{total}: 500 l h^{-1}, τ: 0.500 s, p_{EtOH}: 20 kPa, p_{oxime}: 7 kPa, p_{N2}: 4 kPa, p_{Tol}: 59 kPa, $m_{cat.}$: 24.5 g, $V_{cat.}$: 70 cm^3 and WHSV: 2.9 h^{-1}.

ε-caprolactam selectivity of the unsilylated catalyst after 30 min time-on-stream as compared to the silylated catalyst. The latter observation can possibly be explained by the fact that the unsilylated catalyst contains a significant concentration of unselective isolated silanol groups, while in case of the silylated catalyst these groups were already blocked before the catalytic test.

After longer time-on-stream, in fact already after 15 h time-on-stream the unsilylated catalyst suffered from strong deactivation and additionally from a loss in ε-caprolactam selectivity. To obtain information on the cause for deactivation, weight increase and textural properties of fresh and used catalysts were determined. The results are presented in Table 4. Thereby the unsilylated catalyst gained about 54% weight, while the BET surface area did not change. The assumption that the weight increase is due to coke deposition, suggests that a coke over-layer on the catalyst surface was formed inhibiting access to the active sites. This would finally explain the very low conversion and selectivity after 46 h time-on-stream.

In case of the silylated catalyst the first loss of activity is visible after 29 h time-on-stream. Even after 48 h time-on-stream cyclohexanone oxime conversion decreased only to 93% and ε-caprolactam selectivity remained constant at 90%. The results clearly indicate that silylation reduces catalyst deactivation.

The silylated catalyst shows a very substantial weight increase, although the effect is less than found for the unsilylated catalyst (Table 4). Remarkably, despite 41% weight increase (probably due to coke deposition) the catalytic performance of the silylated catalyst is still very good, indicating that the active sites are still accessible. It should also be noted that this substantial weight increase does not result in a decrease of BET surface area and even resulted in an increase. The very positive effect of silylation is probably related to substantial differences between the silylated and unsilylated catalyst with respect to the distribution of the deposited material over the catalyst particles and/or the properties (density, porosity) of these deposits. Nitrogen physisorption measurements of the used catalyst were carried out to obtain more information on the porosity of the deposited material. Thereby no indication could be found for the presence of meso- and/or micropores in the material deposited on the catalysts. A type II adsorption isotherm is observed up to very high relative pressure without a significant hysteresis effect indicating the absence of mesopores (see Supporting information, Fig. S3). Furthermore, according to the "t-plot" (not shown) no micropores are present.

These observations are in agreement with the fact that the silica support of these catalysts is of a large-pore type with average pore diameter in the macropore range (100 nm diameter accord-

Table 5
Influence of silylation on catalyst water resistance and performance (weight increase, cyclohexanone oxime conversion (X_{5h}), and ε-caprolactam selectivity (S_{5h}), measured after 5 h time-on-stream). Catalyst: 0.5 wt.% Nb_2O_5 loading on DAVICAT SI 1410 silica, particle fraction: 0.85–1.00 mm, 600 °C calcination temperature, L: unsilylated, L1: silylated.

Entry	Catalyst	Ratio water: cyclohexanone oxime[mol:mol]	Weight increase of catalyst [%]	X_{5h} [%]	S_{5h} [%]
1	L	0	6.4	99.9	82.7
2	L	0.5	8.9	99.9	74.7
3	L1	0	2.6	99.9	86.7
4	L1	0.5	1.5	99.9	86.2

Note: Reaction parameters: T_r: 400 °C, p_{in}: 100 kPa, F^g_{total}: 600 l h^{-1}, τ: 0.510 s, p_{EtOH}: 24 kPa, p_{oxime}: 8 kPa, p_{Tol}: 64 kPa, $p_{N2orH2O}$: 4 kPa, m_{cat}: 28.0 g, V_{cat}: 85 cm^3 and WHSV: 3.5 h^{-1}.

ing to the supplier). Considering Table 4 it should be taken into account that the BET surface areas of the used catalysts are given per weight unit of catalyst including the carbonaceous deposits. The contribution of the original catalyst to the BET surface area of the used catalyst can be calculated as shown in Table 4. Furthermore, it should be noted that silica materials can also be described as composed of non-porous spherical particles (average particle diameter of our fresh catalyst can easily be calculated from textural data to be 94 nm).

Thus, from Table 4 and the above considerations we can derive the following simplified picture: the used catalysts contain non-porous large (niobia loaded) silica spheres (with macropores in between) with contributions to the BET surface area of 20.8 $m^2\ g_{used\ cat.}{}^{-1}$ (unsilylated) and 19.8 $m^2\ g_{used\ cat.}{}^{-1}$ (silylated) respectively. The total BET surface area of the used catalysts is higher, 32 $m^2\ g_{used\ cat.}{}^{-1}$ (unsilylated) and 42 $m^2\ g_{used\ cat.}{}^{-1}$ (silylated), resp., as a consequence of the addition of non-porous layers or particles of (carbonaceous) deposits. Models should be found to explain quantitatively the observed increases of BET surface area and weight. For example the following processes might play a role:

1. Carbonaceous particles nucleate at the catalyst surface and grow. If nucleation rate is high with respect to growth rate, many small particles are formed at the surface and total surface area will increase. The small particles may be transformed by growth into a more or less dense layer. Then the original catalyst spheres are enlarged by deposition of a layer of material around the spheres and the surface area will increase by a factor of $(d_{new}/d_{old})^2$.
2. Rate of nucleation is low with respect to growth rate. Then a relatively low concentration of new carbonaceous particles is formed at the catalyst surface, but these grow into the macropores. Total surface area increases, and accessibility of the original surface will remain much better than in case 1.

Possibly a combination of these possibilities will occur. The difference between silylated and unsilylated catalysts might be found in a different relative contribution of these processes. Since the active sites remain accessible for the silylated catalyst, probably process 2 will be relatively more important in this case. It might be that relative rates of nucleation and growth are different depending on silylation due to different hydrophilic–hydrophobic interactions. To decide which factors play a role and to which extent, various analytical techniques have to be applied, e.g. SEM/TEM and mercury porosimetry to determine changes in macropore volume and pore size distribution.

3.4. Effect of silylation treatment on water resistance of the catalyst material

In this Section, the effect of the silylation post treatment on the catalyst water resistance will be discussed. Therefore catalyst L and L1 (properties see Table 5) were tested in a series of experiments under two conditions. First, the reactant gas-phase consisted of toluene, ethanol, cyclohexanone oxime and nitrogen and second, nitrogen partial pressure was substituted by water partial pressure. Table 5 summarizes the results.

When adding water to the substrate solution ε-caprolactam selectivity decreased about 8% in case of the unsilylated catalyst (comparing entries 1 and 2, respectively) whereas the ε-caprolactam selectivity of the silylated catalyst remained constant within experimental error (entries 3 and 4). Water addition has also a different effect on the by-product selectivities of the unsilylated and silylated catalyst. For the unsilylated catalyst both hexanenitrile and cyclohexanone selectivity increase strongly, from nearly 4% to approximately 6% and from 2% to about 4% respectively. In case of the silylated catalyst there is only a weak increase of the cyclohexanone selectivity from 1.1 to 1.6%. The by-products observed could be due to the presence of isolated silanol groups in the unsilylated catalyst, since it has been reported that such groups catalyse the hydrolysis of cyclohexanone oxime with formation of cyclohexanone [46] in combination with the conversion of cyclohexanone oxime to nitriles [47,48].

The presence of isolated silanol groups at the surface was confirmed by FT-IR spectroscopy measurements. The band of isolated surface silanol groups at 3743 cm^{-1} is strongly diminished after silylation. Only the catalytically inaccessible H-bridged internal silanol groups (broad band at ~3666 cm^{-1}) remained and a new peak group appeared originated in the formed trimethylsilyl surface groups (2965 and 2910 cm^{-1}). FT-IR spectra of a silylated and an unsilylated catalyst can be found in the Supporting information in Fig. S4.

The increase of cyclohexanone selectivity upon water addition is in agreement with the presence of groups active for hydrolysis. The much stronger increase in case of the unsilylated catalyst corresponds to the much higher concentration of isolated silanol groups as compared to the silylated catalyst. Another reason for the strong increase of cyclohexanone selectivity due to water addition might be the formation of additional silanol groups. The fact that with the unsilylated catalyst not only the cyclohexanone selectivity increased with water addition but also the hexanenitrile selectivity (while no water is involved directly in the formation reaction) suggests that indeed additional unselective silanol groups were formed. This would occur in particular for the unsilylated but much less or not at all for the silylated catalyst, since rate of rehydroxylation of a silica surface is strongly increased if nuclei of isolated silanol groups are present at the surface, as described by Zhuravlev [54].

Furthermore, there is a significant weight increase of the catalysts during the 5 h tests, as elucidated in Table 5. The nature of these deposits (apart from the observation that the colour of the catalysts turns into black) is not known but probably these consist of carbonaceous deposits ("coke"), or its precursors. Weight increase is much more important for the unsilylated catalyst, suggesting that the isolated silanol groups promote formation of carbonaceous deposits. As an example, heavies could be formed from the cyclohexanone by-product by (acid-catalysed) aldol condensation but also due to polymerization of unsaturated nitriles [55]. Addition of water in case of the unsilylated catalyst results in

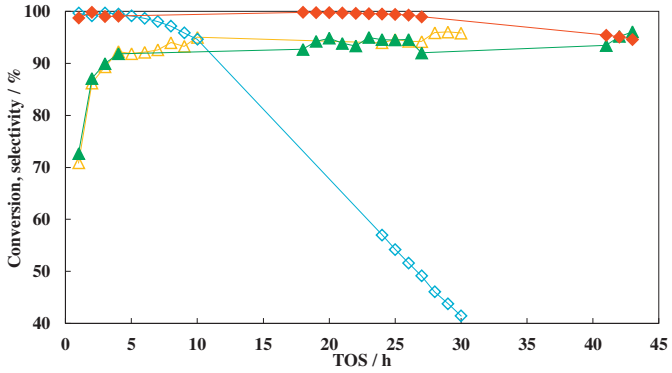

Fig. 5. Catalytic performance, as expressed by the cyclohexanone oxime conversion (◇, ◆ and ε-caprolactam selectivity (△, ▲), of the silylated catalyst M (1 wt.% Nb_2O_5 on DAVICAT SI 1151 silica, 0.25–0.35 mm particle fraction, 600 °C calcination temperature), in the presence (filled symbols) and absence (open symbols) of water in the reactant gas phase, as function of time-on-stream (TOS). Reaction conditions: T_r: 400 °C, p_{in}: 120 kPa, F^{ss}_{total}: 845 l h^{-1}, τ: 0.032 s, p_{EtOH}: 20 kPa, p_{oxime}: 3 kPa, p_{N2}: 1.5 kPa, p_{H2O}: 6 or 0 kPa, p_{Tol}: 89.5 or 95.5 kPa, m_{cat}: 3.0 g, $V_{cat.}$: 8 cm^3 and WHSV: 17.1 h^{-1}.

a still larger weight increase, caused by increased concentrations of by-products. In contrast, addition of water with the silylated catalyst leads to a reduced weight increase, while cyclohexanone selectivity increases slightly. Thus, for the silylated catalyst material there could be two effects caused by water addition, namely:

1. A very slight increase of the hydrolysis rate, the effect being small because of the very low concentration of isolated silanol groups for the silylated catalyst.
2. A decrease of the rate of formation of carbonaceous deposits. Suppression of carbon deposition by water is widely acknowledged and often reported in literature. The decrease is caused for instance by suppression of condensation reactions since water is also product of such a reaction, by decreased acidity/basicity of surface sites as a consequence of water adsorption on these sites or by increased desorption of various organic compounds as a consequence of increased hydrophilicity of the surface.

3.5. Effect of water addition on long-term stability of silylated catalyst

In short-term runs of the silylated catalyst (see Section 3.4) it was demonstrated that the addition of water to the feed reduced the catalyst weight increase during reaction. This finding suggests that addition of water might slow down the deactivation of the silylated catalyst. Therefore the effect of water in the feed on the long-term stability of a silylated catalyst was studied. Silylated catalyst M (1 wt.% niobia, $\rho_A(Nb) = 0.162$ Nb nm^{-2}, 600 °C calcination temperature) was prepared using DAVICAT SI 1151 silica with a particle fraction of 0.25–0.35 mm.

Fig. 5 presents the results of the long-term runs without and with water in the reactant gas-phase. As a consequence of water addition the catalytic long-term stability is enhanced very substantially: The period over which the conversion decreases from >99% to 94% increases from 10 h time-on-stream to 43 h time-on-stream. This result is reflected in the amount of coke deposition. The relative weight increase of the catalyst during reaction in presence of added water was about 38% and thus 12% lower than the observed 50% weight increase of the catalyst without water addition. A similar observation has been made before in the case of zeolite-catalysed GPBR [33]. Note that the silylation treatment has increased the stability of the catalytic performance to water to such an extent that water can even be added to increase the catalytic long-term stability.

When comparing these results to the results of Section 3.4 (Figs. 4 and 5) it can be seen that the silylated catalyst M deactivates faster than catalyst L1. To explain this, the following considerations have to be taken into account:

1. For catalyst M a much higher WHSV was applied, WHSV = 17.1 h^{-1} compared to 2.9 h^{-1} for catalyst L1. Thus the conditions were much more demanding in case of catalyst M. In fact catalyst M was operated at a higher productivity of 41.7 mmol kg^{-1} s^{-1} ($X_{25\,h}$ = 99.4%) compared to 7.1 mmol kg^{-1} s^{-1} ($X_{25\,h}$ = 99.6%) for catalyst L1, at 25 h time-on-stream.
2. The average pore diameter for catalyst M was only about 1/10 of that of catalyst L1. The smaller pores get possibly more easily blocked by carbonaceous deposits leading to faster deactivation.

Summarizing, the results from Sections 3.3 and 3.4 show that catalyst lifetime can be increased strongly by silylation and by water addition. The results also suggest that the final lifetime achieved depends on reaction conditions and on texture and thus further optimization should be possible.

Additionally it should be stressed that catalyst M was tested under a reactor inlet pressure of 120 kPa and an atmospheric reactor outlet pressure representing more favourable conditions for a possible industrialization because with the vacuum pump (P3 in Fig. S1) can be dispensed. Both aspects underline the improvements of the catalyst and reaction parameter optimization.

3.6. Comparison of the performances of NbO_x/SiO_2 and silicalite as GPBR catalyst

Comparison of the catalytic performances of our NbO_x/SiO_2 catalyst and the Sumitomo GPBR catalyst (silicalite), considered as benchmark, is not straightforward because of the very different reactor types used (fixed bed versus fluidized bed) and because of the continuous catalyst regeneration applied by Sumitomo [15]. Nevertheless from the Sumitomo patent example [15] follows that the fluidized bed system (with continuous regeneration) yields, for a WHSV of 5.0 h^{-1}, a constant cyclohexanone oxime conversion of 99.6% and ε-caprolactam selectivity of 95.7%. From the given patent examples an ε-caprolactam productivity of about 12 mmol kg^{-1} s^{-1} can be estimated (350 °C reactor temperature). Our NbO_x/SiO_2 catalyst in a fixed bed displays (see previous section), during a period of about 26 h time-on-stream, a constant cyclohexanone oxime conversion >99% and a constant ε-caprolactam selectivity of 95% for a WHSV of 17.1 h^{-1}, corresponding to an ε-caprolactam productivity of about 40 mmol kg^{-1} s^{-1} (400 °C reactor temperature).

Recently, Xing et al. [56] reported results of a study on GPBR applied in a fixed bed reactor system over silicalite as catalyst operated at atmospheric pressure. From the results a productivity of about 24 mmol kg^{-1} s^{-1} can be estimated (385 °C reactor temperature).

Taking this all together, it can be concluded that the catalytic performance of the optimized NbO_x/SiO_2 catalyst material is in a comparable range with the silicalite catalyst used by Sumitomo.

4. Conclusions

NbO_x/SiO_2 was successfully optimized for the gas-phase Beckmann rearrangement in terms of catalytic performance and regarding to process technological aspects. Investigations of the effects of calcination temperature and niobia loading lead to the conclusion that the catalytic performance is optimal for a catalyst

calcination temperature of 600 °C and a niobia loading of 0.3 wt.%. The presence of niobia is essential for high catalytic performance, as follows from the very low activity and ε-caprolactam selectivity observed for the silica support without niobia. Raman spectroscopy results reveal that these NbO_x/SiO_2 materials contain isolated tetrahedral mono-oxo NbO_4 surface species, which most probably play an essential role in the catalytic performance. Catalyst materials with different niobia loadings, calcined at 600 °C, showed a linearly increasing catalytic activity up to 0.3 wt.% Nb_2O_5. For loadings higher than 0.3 wt.% a decrease of activity was observed, most probably due to agglomeration of NbO_4 surface sites. A HMDS silylation post-treatment of the catalyst material, transforming unselective isolated silanol groups into hydrophobic trimethylsilyl groups, had very positive effects. Firstly, the long-term stability of a silylated catalyst increased very substantially. This is most probably mainly the consequence of a different distribution of the deposited coke over the surfaces of catalytic materials. Thereby a much larger fraction of original surface remains accessible for the silylated than for the unsilylated catalyst material. Secondly, the silylation post-treatment suppresses the harmful effect of water on the ε-caprolactam selectivity, thereby enabling water addition to the feed in order to enhance the catalytic long-term stability. The positive effect of water addition on the long-term stability of a silylated catalyst was clearly demonstrated for rather demanding conditions (high WHSV and high reactor pressure). Water addition increased the period over which conversion decreases from >99 to 94% by a factor of four at constant ε-caprolactam selectivity about 95% over the full period. Summarizing, the possibility to operate at high space velocities and reactor pressures ≥100 kPa (absolute), while obtaining a high conversion, a relatively low deactivation rate and constant high ε-caprolactam selectivity is an important improvement compared to previous studies of these niobia catalysts. Considering the only industrial gas-phase Beckmann rearrangement process of Sumitomo as benchmark, the catalytic performance of both systems in terms of activity, selectivity and productivity is in a comparable range. The results presented suggest that the NbO_x/SiO_2 catalyst material described in this work has the potential for further optimization, which offers perspectives for a future gas-phase Beckmann rearrangement process in a fixed bed reactor.

Acknowledgements

M. Maronna thanks DSM for financial support as well as for providing the laboratory facilities for executing the work. The authors are grateful to Dr. S. Küppers, Dr. H. Lippert and Dr. S. Tückhardt (Forschungszentrum Jülich ZEA-3 Analytik, Germany) for ICP-MS measurements, Dr. J. Dornseiffer (Forschungszentrum Jülich, IEK-1, Germany) for applying N_2-adsoption analysis and F. Schmidberger from Grace Davison (Germany) for providing the silica materials.

Appendix A. Supplementary data

Supplementary data associated with this article can be found, in the online version, at http://dx.doi.org/10.1016/j.apcatb.2015.12.014.

References

[1] G. Dahlhoff, J.P.M. Niederer, W.F. Hoelderich, Catal. Rev. 4 (2001) 381–441.
[2] W., Lazier, G., Rigby, Patent US 2234566, assigned to Du Pont, 1941.
[3] Patent FR 857714A, assigned to DuPont, 1940.
[4] Patent FR 892603A, assigned to Deutsche Hydrierwerke AG, 1944).
[5] W., Hentrich, K., Stickdorn, Patent DE 919047C, assigned to DEHYDAG, 1954.
[6] O., Drossbach, H., Hopff, Patent DE 741038C, assigned to IG Farben, 1943.
[7] W. Dawydoff, Chem. Technol. 11 (1955) 647–655.
[8] G.P. Heitmann, G. Dahlhoff, W.F. Hoelderich, Appl. Catal. A Gen. 185 (1999) 99–108.
[9] W.F. Hoelderich, J. Röseler, G. Heitmann, Catal. Today 37 (1997) 353–366.
[10] J. Röseler, G. Heitmann, W.F. Hoelderich, Appl. Catal. A Gen. 144 (1996) 319–333.
[11] W.F., Hoelderich, J., Roeseler, D., Arntz, Patent US 5741904, assigned to Degussa, 1998.
[12] Y. Izumi, H. Ichihashi, Y. Shimazu, Bull. Chem. Soc. Jpn. 7 (2007) 1280–1287.
[13] H. Ichihashi, M. Kitamura, Catal. Today 73 (2002) 23–28.
[14] H. Ichihashi, H. Sato, Appl. Catal. A Gen. 221 (2001) 359–366.
[15] M., Kitamura, Y., Schimazu, Patent US 6265574B1, assigned to Sumitomo, 2001.
[16] T. Ushikubo, K. Wada, J. Catal. 148 (1994) 138–148.
[17] K. Sugiyama, G. Anan, T. Ushikubo, Surf Coatings Technol. 112 (1999) 76–79.
[18] S.K. Pillai, O. Gheevarghese, S. Sugunan, Appl. Catal. A Gen. 353 (2009) 130–136.
[19] S. Mandal, C. Santra, R. Kumar, RCS Adv. 4 (2014) 845–854.
[20] M.H. Kim, Y. Ko, S.J. Kim, Appl. Catal. A Gen. 210 (2001) 345–353.
[21] S.J. Kim, K.D. Jung, O.S. Joo, Stud. Surf. Sci. Catal. 154 (2004) 2815–2822.
[22] M. Anilkumar, W.F. Hoelderich, J. Catal. 260 (2008) 17–29.
[23] M. Anilkumar, W.F. Hoelderich, Catal. Today 198 (2012) 289–299.
[24] M. Anilkumar, W.F. Hoelderich, J. Catal. 293 (2012) 76–84.
[25] PhD dissertation Anilkumar Mettu RWTH Aachen University, 2009.
[26] M. Anilkumar, W.F. Hoelderich, Appl. Catal. B Environ. 165 (2015) 87–93.
[27] M. Kitamura, H. Ichihashi, Stud. Surf. Sci. Catal. 90 (1994) 67–70.
[28] H. Sato, K. Hirose, M. Kitamura, Stud. Surf. Sci. Catal. 49 (1989) 1213–1222.
[29] A. Bordoloi, S.B. Halligudi, Appl. Catal. A Gen. 379 (2010) 141–147.
[30] J. Kim, W. Park, R. Ryoo, ACS Catal. 1 (2011) 337–341.
[31] F. Meng, Y. Wang, R. Yang, J. Mol. Catal. A Mol. 335 (2011) 105–111.
[32] C.C. Pavel, R. Palkovits, F. Schüth, J. Catal. 254 (2008) 84–90.
[33] J. Röseler, G. Heitmann, W.F. Hoelderich, Appl. Catal A Gen. 144 (1996) 319–333.
[34] M.M., Maronna, E.C., Kruissink, W.F., Hoelderich, Unpublished results.
[35] E.L. Lee, I.E. Wachs, J. Phys. Chem. C 111 (2007) 14410–14425.
[36] E.L. Lee, I.E. Wachs, J. Phys. Chem. C 112 (2008) 6487–6498.
[37] B.M. Weckhuysen, J.M. Jehng, I.E. Wachs, J. Phys. Chem. B 104 (2000) 7382–7387.
[38] I.E. Wachs, L.E. Briand, J.M. Jehng, Catal. Today 57 (2000) 323–330.
[39] L.J. Burcham, J. Datka, I.E. Wachs, J. Phys. Chem. B 103 (1999) 6015–6024.
[40] C.B. Wang, Y. Cai, I.E. Wachs, Langmuir 15 (1999) 1223–1235.
[41] G. Deo, A.M. Turek, I.E. Wachs, Zeolites 13 (1993) 365–373.
[42] Y. Borodko, J.W. Ager, G.E. Marti, J. Phys. Chem. B 109 (2005) 17386–17390.
[43] X. Gao, S.R. Bare, B.M. Weckhuysen, I.E. Wachs, J. Phys. Chem. B 102 (1998) 10842–10852.
[44] R.H. Stolen, G.E. Walrafen, J. Chem. Phys. 64 (1976) 2623–2630.
[45] J.C. Mikkelsen, F.L. Galeener, W.J. Mosby, J. Electron. Mater. 10 (1981) 631–651.
[46] M.A. Camblor, A. Corma, H. Garcia, J. Catal. 177 (1998) 267–272.
[47] R. Maheswari, K. Shanthi, T. Sivakumar, Appl. Catal. A Gen. 248 (2003) 291–301.
[48] D. Shouro, Y. Ohya, S. Mishima, Appl. Catal. A Gen. 214 (2001) 59–67.
[49] P.A. Burke, E.I. Ko, J. Catal. 129 (1991) 38–46.
[50] S.M. Maurer, E.I. Ko, Catal. Lett. 12 (1992) 231–238.
[51] J.M. Jehng, I.E. Wachs, Catal. Today 16 (1993) 417–426.
[52] J.M. Jehng, I.E. Wachs, J. Mol. Catal. 67 (1991) 369–387.
[53] J. Datka, A.M. Turek, J.M. Jehng, I.E. Wachs, J. Catal. 135 (1992) 186–199.
[54] L.T. Zhuravlev, Coll. Surf. A 173 (2000) 1–38.
[55] P. Albers, K. Seibold, T. Haas, W.F. Hoelderich, J. Catal. 176 (1998) 561–568.
[56] J. Xing, M. Fanhui, W. Shuhai, W. Yaquan, CIESC J. 64 (2013) 924–930.